JOURNAL OF AIRCRAFT
Vol. 39, No. 2, March–April 2002

Flight-Path Management/Control Methodology to Reduce Helicopter Blade–Vortex Interaction Noise

Fredric H. Schmitz,* Gaurav Gopalan,† and Ben Wel-C. Sim‡
University of Maryland, College Park, Maryland 20742

A quasi-static acoustic mapping method has been developed to predict rotorcraft external noise. This method takes advantage of an expansion, to first order, about a solution to the helicopter nondimensional steady-state trim equations to include the effects of acceleration parallel to the flight path and *X*-force control changes on the radiated noise. Application of the new method to predict helicopter blade–vortex interaction (BVI) noise has shown that choice of flight-path angle, *X*-force, and vehicle acceleration all have an important influence on ground noise exposure during approach and landing. The effect of constant flight-path-angle approaches on BVI ground noise, with and without *X*-force control, is compared with decelerating approaches at the same flight-path angle. Two different quiet flight trajectories are suggested that use a combination of these controls to minimize BVI noise exposure on the ground during a helicopter approach to a landing.

Nomenclature

A_{sph}	=	radiation sphere total area
A_x	=	acceleration parallel to flight path
a_0	=	speed of sound, 1125 ft/s
C_T	=	thrust coefficient
c	=	rotor blade chord
D_f	=	rotor drag
d	=	blade-to-vortex separation distance
F_x	=	auxiliary X force
f	=	equivalent flat plate drag area of the helicopter
f_x	=	equivalent flat plate area of X-force device
g	=	gravity constant, 32.2 ft/s^2
M_{ht}	=	hover-tip Mach number, $\Omega R/a_0$
P_{av}	=	average acoustic power on sphere
R	=	rotor blade radius
R_{obs}	=	hub-to-observer distance
t	=	time
t_{obs}	=	observer time
V	=	helicopter velocity
v	=	rotor induced velocity
W	=	helicopter weight
x, y	=	ground plane coordinates
x_{tpp}, y_{tpp}, z_{tpp}	=	tip-path-plane coordinates
α_{tpp}	=	tip-path-plane angle (positive nose up)
γ	=	flight-path angle (negative in descent)
θ	=	radiation sphere elevation angle
λ	=	average rotor inflow (positive for upwash)
μ	=	advance ratio, $V/\Omega R$
ρ	=	density of air, 0.002378 slugs/ft^3
τ_{source}	=	source time
ψ	=	radiation sphere azimuth angle
Ω	=	angular rotation

Received 25 March 2000; revision received 11 September 2001; accepted for publication 13 September 2001.

*Martin Professor of Rotorcraft Acoustics, Aerospace Engineering Department. Fellow AIAA.

†Graduate Research Assistant, Aerospace Engineering Department. Student Member AIAA.

‡Assistant Research Scientist, Aerospace Engineering Department. Member AIAA.

Introduction

WHEN it occurs, blade–vortex interaction (BVI) noise is one of the most distinct and objectionable sounds emitted from rotorcraft. Its typical popping or slapping sound radiates large amounts of acoustic energy in distinct patterns far from its source. BVI noise occurs mostly during landing/descending flight, and sometimes in maneuvering flight, when the rotating blades pass in close proximity to the previously shed rotor tip vortices. These vortices induce sharp periodic aerodynamic disturbances on the blades (higher harmonic blade loading), which generate highly impulsive BVI noise. The radiated noise is dependent on the miss distance between the rotor blades and the previously shed vortex system, the geometry of each particular vortex encounter, and several governing nondimensional parameters.[1–5]

This paper focuses on the use of piloting techniques and auxiliary controls to reduce BVI noise. It concentrates on the landing/descent phases of flight of a helicopter that is operating near or in a noise sensitive community. Some of the first experimental attempts at using flight-path control to reduce the noise exposure to the surrounding community were done by Hawles.[6] By the use of cabin noise measurements and subjective evaluations of those measurements, a "fried egg" region was approximated for particular helicopters on a rate of sink vs forward velocity plot shown in Fig. 1. The pilot was to avoid this region, and in so doing, would minimize BVI noise radiation to the surrounding community. These procedures were developed into the "Fly Neighborly Program,"[7] which has helped minimize BVI noise radiation for certain helicopters. More recent experimental flight testing using GPS tracking and guidance has shown that flight trajectory control can alter helicopter noise exposure to the surrounding community.[8]

Early theoretical attempts at using flight-path management to minimize noise radiation for vertical takeoff and landing aircraft showed that trajectories did exist that could help mitigate the noise problem.[9] Mathematical models of aircraft performance and noise generation/radiation were developed and used to project noise exposure to the surrounding communities.[10,11] In these early studies, it was also discovered that BVI aerodynamic and noise modeling did not have the necessary mathematical fidelity to represent adequately the physics of the BVI phenomena. More recent theoretical studies have used flight and wind-tunnel acoustic data together with estimates of flight performance to estimate the likelihood of BVI noise radiation.[12,13]

Recent attempts at predicting the noise radiation to the ground from a helicopter flying a specified flight trajectory have used a rotor noise model (RNM).[14] Instead of directly calculating the noise, this approach maps acoustic data that have been stored as a function

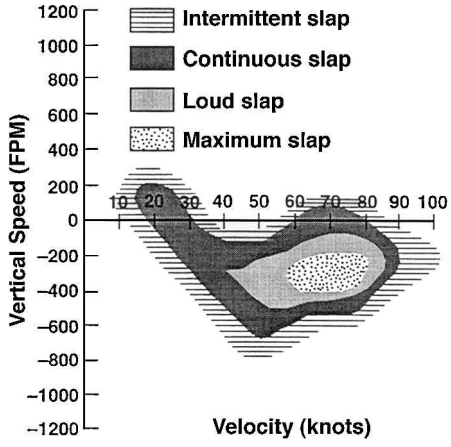

Fig. 1 Measured cabin noise levels as a function of helicopter flight conditions (Ref. 6).

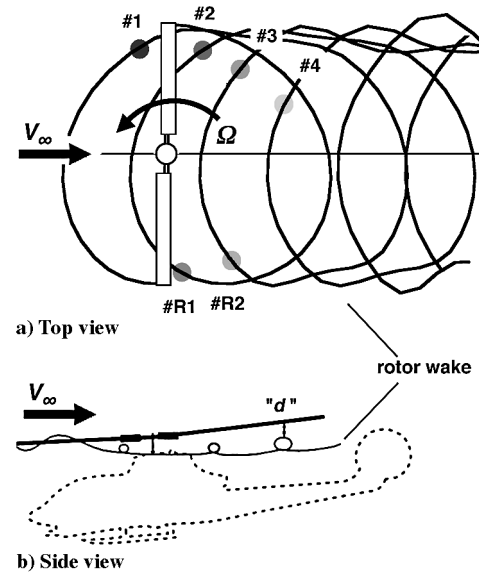

Fig. 2 Helicopter BVI geometry for a two-bladed rotor.

of steady-state flight conditions of the helicopter, to observers on the ground. Work to date has been promising. However, the effects of acceleration and other parameters that can alter the vehicles performance state have not been included in RNM noise predictions.

BVI aerodynamic and acoustic modeling have dramatically improved over the past 25 years. It is now possible to predict more accurately many of the features of BVI noise radiation with more certainty, especially if measured blade loading is used as input to the noise radiation calculations. The general BVI directivity characteristics of the radiated noise as a function of several design parameters have been explored for several types of rotorcraft.[3–5,15–19] Comparisons between experiment and theory have been encouraging. If measured pressures are used as input to the acoustic equations, the predictions capture many of the features of BVI noise.

This paper attempts to capitalize on these improvements in understanding and prediction methods and to use them to explore flight-path and configuration management options that will minimize helicopter BVI noise radiation and exposure on the ground. It uses the performance modeling, developed by Schmitz,[12] to approximate the effect of acceleration and X force on the rotor tip-path-plane angle and coupling the tip-path-plane angle prediction with a variation of the RNM acoustic mapping method,[14] to project the noise to the ground. The result is a new prediction method called quasi-static acoustic mapping (Q-SAM). Although the Q-SAM method is general, as in Ref. 12, it is applied to the Bell Helicopter Textron's AH-1 Cobra helicopter for the final calculations presented in this paper. Several constant velocity flight-path noise exposure profiles are explored. Finally, the new method is used to present two helicopter configurations and/or descent profiles that reduce the noise exposure for the AH-1 series helicopter.

Helicopter Noise/Performance Modeling

Predicting BVI noise from rotorcraft, especially one that is maneuvering in space, is quite a challenging proposition. It requires a high-fidelity comprehensive mathematical modeling of the aerodynamics and dynamics of the helicopter, as well as comprehensive modeling of BVI acoustic sources. Although certain aspects of this modeling are under development, a comprehensive mathematical model that can predict the noise from first principle approach for a maneuvering helicopter is not yet available. Instead, rotorcraft BVI noise prediction has focused on predicting the radiated noise over a series of steady-state flight conditions. These predictions are often validated in specially developed anechoic wind tunnels and/or acoustic flight tests.

Under trimmed steady-state flight, it has been shown that BVI noise is governed by four helicopter nondimensional variables;[1] rotor thrust coefficient C_T, rotor advance ratio μ, rotor tip-path-plane angle α_{tpp}, and hover-tip Mach number M_{ht}. The geometry of the BVI problem is shown in Fig. 2 for a two-bladed helicopter as seen from a top and a side view. In the top view, rotor blades appear to intersect the tip vortices that were previously shed from the tips of the rotor at earlier times. For a fixed number of blades, the number of these vortex interactions is determined by the rotor advance ratio. The top view also shows that the BVI event often sweeps along the blade effectively causing unsteady aerodynamic disturbances. These disturbances radiate a portion of their energy as acoustic waves. Under some conditions, these acoustic waves are summed in phase to amplify the BVI noise radiated in certain directions and locations far from the rotor. This linear wave collection process is governed by the trace Mach number time history, which is known to be a function of the hover-tip Mach number and advance ratio. The importance of the trace Mach number on the strength and directivity of BVI radiation has been reported in Refs. 15–19, and will not be repeated here.

The miss distances d between the shed vortices and the rotor blades during BVI are shown in the side view (Fig. 2b). The strength of the shed vortices and the miss distances are also controlled by the same four nondimensional parameters in trimmed steady-state flight. The actual aerodynamic events that determine the quantitative levels of BVI noise, even in trimmed steady-state flight, are quite complicated. Comprehensive mathematical models of rotorcraft have been developed that attempt to model these and other physical effects of the rotor and wake on the blade aerodynamic loading.[20,21] The results that are derived from these models are dependent on details of the rotor wake structure that are not easy to predict very accurately. The mathematical modeling is most accurate when important empirical factors are chosen by comparing the modeling with experimental measurements at selected performance conditions. These parameters are then used to extrapolate the predictions to other rotorcraft performance states.

This paper focuses at a subset of the maneuvering helicopter problem, quasi-static performance, which consists of a sequence of slowly evolving performance state changes. Helicopter performance conditions are limited to slow accelerations ($|A_x| \leq 0.1\,g$) in the longitudinal plane and conventional approach angles ($|\gamma| \leq 10$ deg). The effect of changing flight-path angles, $\mathrm{d}\gamma/\mathrm{d}t$, is also neglected in this simplified performance model. These assumptions and constraints are well within the bounds that are normally used in an approach to a landing for commercial helicopter operations. In addition, when small-angle assumptions are used, the small force in the tip-path-plane of the rotor[12] in moderate-speed flight is neglected, and that the thrust equals weight is assumed, the X-force balance equation in a wind axis system is [Eq. (15) from Ref. 12]

$$\alpha_{\text{tpp}} = -\frac{D_f}{W} - \gamma - \frac{1}{g}\left[\frac{\mathrm{d}V}{\mathrm{d}t}\right] - \frac{F_X}{W} \tag{1}$$

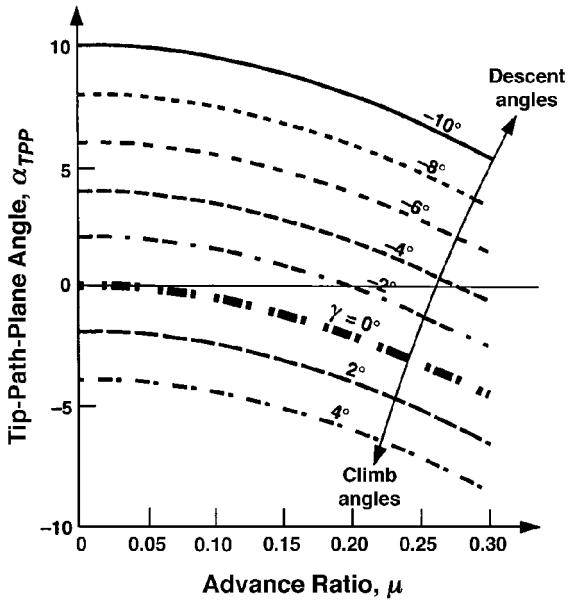

Fig. 3 Tip-path-plane angle vs advance ratio for different flight path angles (Ref. 12).

where

$$D_f = \tfrac{1}{2}\rho V^2 f, \qquad F_X = \tfrac{1}{2}\rho V^2 f_X$$

(Note that the wind axis system becomes ill defined at very low-speed flight. As a consequence, it is assumed that this analysis is valid for forward velocities of 40 kn or greater.)

With these assumptions, this first-order nonlinear differential equation governs the force balance of the helicopter. The equation contains an auxiliary X force[12] F_X that can be used to directly control the helicopter's tip-path-plane angle. For this paper, only aerodynamically generated X force is considered, making the X force dependent on the square of the velocity.

If it is further assumed that acceleration parallel to the flight path is zero and there is no X force ($F_X = 0$), the resulting algebraic equation describes the steady-state longitudinal performance of the helicopter:

$$\alpha_{\text{tpp}} = -D_f/W - \gamma \tag{2}$$

The rotor's tip-path-plane angle [Eq. (2)] simply becomes a function of the forward velocity, descent angle, vehicle gross weight, and the total vehicle wetted area drag coefficient. The resulting tip-path-plane angle for the AH-1 helicopter vs forward velocity is shown in Fig. 3 for several steady-state climb angles. Climbing flight decreases α_{tpp}, whereas descending flight increases α_{tpp}.

In this steady-state model of helicopter performance, the rotor tip-path-plane angle and the vehicle velocity represent the trim states of the helicopter. With the helicopter thrust and hover-tip Mach number usually held nearly constant during the landing phase of flight, the helicopter trim is effectively governed by the tip-path-plane angle α_{tpp} and the advance ratio μ of the helicopter. At each trim state of μ and α_{tpp} obtained for a given C_T and M_{ht} representative of the helicopter in flight, these nondimensional parameters also define the BVI aerodynamics and the resulting BVI noise radiated by the rotor.[1] This relationship was shown in an approximate way in Ref. 12 through the calculation of an average rotor inflow. When the average inflow to the rotor is near zero, strong BVI is likely.

Expanding this set of steady-state trim solution space to include small accelerations along the flight path is a straightforward procedure but it is quite important for realistic performance modeling for acoustic predictions. As seen in Eq. (1), acceleration parallel to the flight path acts quite similarly to changes in climb angle: Acceleration decreases α_{tpp} (becoming more negative) and deceleration effectively increases α_{tpp}.

If we now assume that acceleration parallel to the flight path, A_x, is a trajectory control variable, Eq. (1) reduces to the algebraic equation

$$\alpha_{\text{tpp}} = -D_f/W - (\gamma + A_X/g + F_X/W) \tag{3}$$

In effect, acceleration has been redefined as another parametric control. This new algebraic equation (3) can be solved for any choice of acceleration, flight-path angle, and X force, as a function of flight velocity. This procedure of treating acceleration as another parameter in a steady-state solution procedure is called quasi-static performance prediction and is used throughout this paper. Because acceleration, flight-path angle, and X force have the same functional form in Eq. (1), further conceptual simplifications are allowed. It reduces the algebraic solution for tip-path-plane angle to again be a function of two variables, helicopter effective drag and the sum of flight-path angle, acceleration along the flight path, and X force.

The implications of using this quasi-static performance prediction approach for acoustics are substantial. For a given helicopter operating on a standard day at a given gross weight, the tip-path-plane angle is specified algebraically by choosing some combination of flight-path angle, acceleration along the flight path, and X force. In essence, the acceleration and X force control are equivalent to flight-path angle control changes, and the combined $(\gamma + A_x/g + F_x/W)$ term can be treated as an equivalent climb angle.[12] Acceleration parallel to the flight path and X force simply determine a different trim location on the steady-state tip-path-plane angle vs velocity performance map shown in Fig. 3.

Ground Noise Modeling

As discussed in the Introduction, BVI noise prediction requires the detailed blade loading time history for each rotor blade. This can be provided by directly solving the set of nonlinear differential equations that govern rotorcraft flight. The output of the performance model provides the detailed blade loading time histories, which, along with other flow and rotor parameters, become the input to the governing BVI acoustic equations of the helicopter. For the most part, the governing acoustic equations are based upon the Ffowcs-Williams and Hawkings integral equation.[22] Solutions are not trivial because the governing aerodynamics are quite complicated and often nonlinear. For BVI, only the linear unsteady pressure terms are normally used for the linear calculation of the resulting noise.[23] This direct approach was used in Ref. 9 to calculate the noise of a tiltrotor aircraft performing several near-optimal noise abatement trajectories and in Ref. 24 to examine the noise from maneuvering helicopters. Attenuation, spherical spreading, and noise weighting effects are included as a part of the direct approach calculations. As discussed earlier, these calculations are critically dependent on the fidelity of the rotor aerodynamics.

It is also possible to use an acoustic mapping approach to predict the radiated noise. Here, it is implicitly assumed that the accelerations parallel and perpendicular to the flight path and X force are zero ($A_x = 0$ and $F_x = 0$). The governing steady-state performance and acoustic equations are solved, projecting the noise radiation patterns to a large number of points on the surface of a radiation sphere that surrounds the effective emission point(s) of the noise source(s). This is done for each steady-state trim state of the rotor and is stored for further calculations. The calculation of noise for a particular trajectory is accomplished by piecing together a series of trajectory elements and mapping the corresponding noise levels on these radiation spheres to chosen points along the ground. Atmospheric attenuation, spherical spreading, noise weightings, etc., are included in the mapping procedure. This approach is being used by the rotorcraft community to try to estimate the noise generated by rotorcraft flying near affected communities.[14]

The acoustic mapping approach has several advantages. Because it relies on only the steady-state trim conditions of the rotorcraft, radiated noise can be stored on spheres in a relatively small parameter space as a function of μ and α_{tpp} (Ref. 14 uses V and γ). These radiation sphere acoustics can be calculated directly from first principle relationships, or they can be obtained from direct steady-state

trim acoustic measurements of helicopters. (The latter technique can take advantage of ground-based measurements, wind-tunnel measurements, or in-flight acoustic measurements to assess the different components of radiated noise.) The major advantage of using the measured acoustic data in the acoustic mapping approach is that the complex aerodynamic processes that govern BVI can be accurately captured for each steady-state performance condition. However, the acoustic mapping approach has one big disadvantage: It neglects the effect of vehicle acceleration on the radiated noise, a factor that is very important for BVI noise prediction.

Q-SAM Method

A new method is proposed in this paper that capitalizes on the advantages of quasi-static performance modeling of the rotor performance states and the acoustic mapping approach. It is the Q-SAM method and is conceptually shown in Fig. 4. Spherical distributions of radiated noise are first developed and stored as a function of α_{tpp} and μ for the trim states of the helicopter, $\mathrm{d}V/\mathrm{d}t = 0$ and $F_X = 0$. This is schematically shown on the left side of Fig. 4. The quasi-static tip-path-plane angle is then calculated for each element along the trajectory according to Eq. (3), as shown on the right side of Fig. 4. Noise radiated from each trajectory element is found by interpolating in μ and α_{tpp} space and using the quasi-static value of α_{tpp}. A spherical distribution of noise (radiation sphere) is obtained for each segment of the trajectory. This radiation sphere is then used to map noise to selected positions along the ground. The time history at any position on the ground is found by summing the noise radiated from each segment of the trajectory.

The Q-SAM approach to performance and noise prediction modeling presented here can work with many levels of aerodynamic modeling, from very sophisticated analyses incorporating free-wake and compressible flow calculations, to simple prescribed wake methods. It is also possible to use measurements of acoustic data sets that surround the rotor, thus avoiding prediction of the noise altogether. Because the measured acoustic data already incorporate many of the finer details of the aerodynamics that generate BVI noise, the fidelity of this approach can, in some cases, be superior to the comprehensive mathematical modeling approach.

In its present state of development, the Q-SAM method uses theory to develop the radiation spheres and incorporates the important effect of acceleration along the flight path in the acoustic predictions. The method is most accurate for small accelerations, which are typical for helicopter landing/approach trajectories.

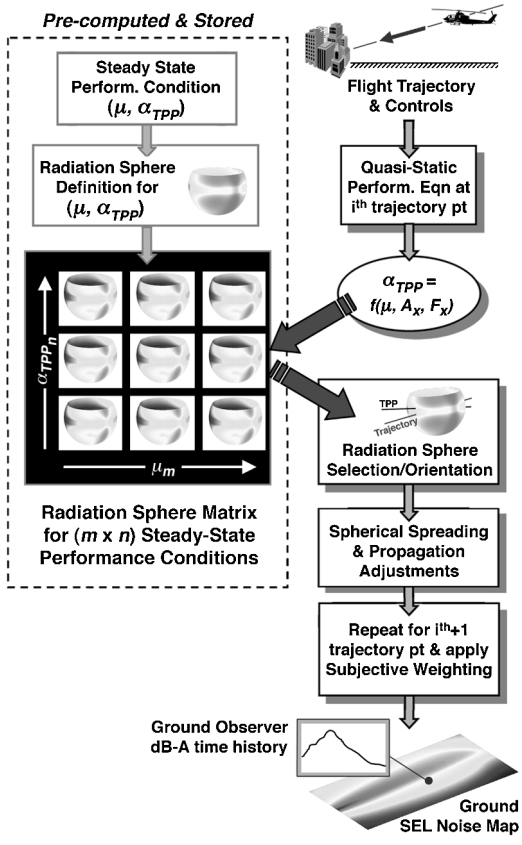

Fig. 4 Ground noise calculation: Q-SAM method.

Application of the Q-SAM Method to the AH-1 Helicopter

The advantages of using the Q-SAM method to predict BVI noise radiated to the ground in approach/landing phases of flight are illustrated by application to the AH-1 Cobra helicopter. The AH-1 was selected because the authors are quite familiar with its performance and acoustic characteristics and because much of the rotor's BVI noise characteristics has been reported in the open literature. The rotor geometry and operational parameters are summarized in Table 1.

The Q-SAM method requires an initial acoustic mapping surface or surfaces to be located far enough away from the noise source or sources to capture the far-field acoustic radiation characteristics of the rotorcraft. This requirement ensures that near-field acoustic source strengths are small when compared to sources that propagate acoustic energy away from the rotor.[25] However, these large distances can make the pressures recorded or measured on the mapping surface, due to these radiating sources, small. In addition, some portions of a chosen flight trajectory might bring the rotorcraft quite close to the ground, where the mapping surface distance could be larger than the distance between the position of the effective sound source and observer positions on the ground. Another important consideration is that in an approach to a landing, the aircraft is often at low altitudes and far away from the observer locations. This geometry causes energy to be radiated at near in-plane positions and requires that the radiation surface accurately represent these radiation zones. Accuracy is also sacrificed by real-world events such as wind and temperature effects, ground reflection, and atmospheric absorption. These issues deserve careful consideration before the Q-SAM method is used with measured acoustic data.

To accommodate many of these concerns, the mapping surface in this paper is chosen to be a radiation sphere centered on the acoustic event in inertial space and located 25 rotor radii from its effective source point (Fig. 5). The spherical shape allows the radiation sphere to capture the complete directivity of the noise and also facilitates the projection of that directivity to positions on the ground plane. The large distance from the effective source point ensures that this radiation sphere only captures far-field acoustic radiation. Once the far-field acoustic radiation is captured (or predicted) on the radiation sphere, it can be related to larger or smaller radiation spheres by using far-field scaling laws that also account for the effects of atmospheric corrections.

Table 1 AH-1 helicopter geometry and flight parameters

Parameter	Symbol	Value
	AH-1 helicopter	
Number of blades	N	2
Blade radius	R	22 ft
Blade chord	c	2.2 ft
Angular rotation	Ω	324.35 rpm
Hover-tip Mach number	M_{ht}	0.664
Thrust coefficient	C_T	0.0054
Equivalent flat plate area	f	14 ft^2
Helicopter weight	W	10,600 lb
	Descent	
Advance ratio (velocity)	$\mu(V)$	0.120 (53 kn)–0.210 (93 kn)
Flight-path angle	γ	−2 to −9 deg
X-force equivalent flat plate area	f_x	14 ft^2
Deceleration	A_x	0.05 g, 0.10 g

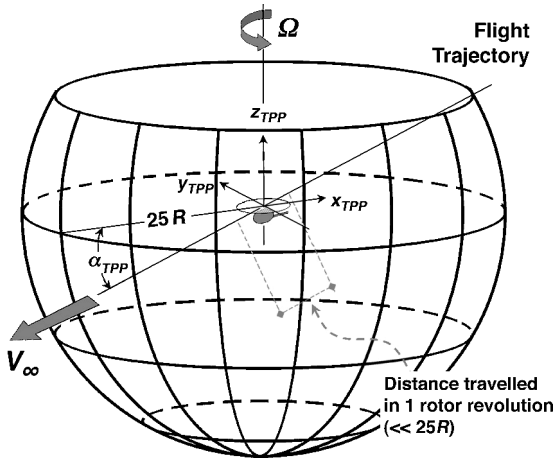

Fig. 5 Radiation sphere used in the Q-SAM method.

BVI Noise Prediction on Radiation Sphere

In principle, the information on the radiation sphere can be derived from either experimental measurements, or theoretical noise prediction codes, or both. For the AH-1 calculations illustrated in this section, this information is generated by analyses similar to the methods used in Ref. 15 for wind-tunnel BVI noise comparisons. Appropriate modifications were introduced to the calculation of retarded time to predict ground observer noise. The analysis utilizes a prescribed wake system[26,27] to estimate the local unsteady rotor blade airloads due to BVI. The predicted airloads are then used as input to an acoustic formulation/code,[28] which predicts the level and directivity of the noise on the radiation sphere at 5-deg intervals, in both the azimuth and elevation angle directions.

Although it is acknowledged that unsteady three-dimensional aerodynamics can be quite important for accurately predicting impulsive BVI events, the airloads are evaluated in this paper by using only quasi-steady, two-dimensional aerodynamics (strip theory). This simplified modeling was found to provide generally good agreement in the BVI noise level and directivity trends for the AH-1 helicopter.[15] It is expected that the same modeling would be good enough to discern the changes in BVI noise due to changes in the rotor's operating states.

Because of the known sensitivity of BVI acoustics to wake modeling effects, two wake models were explored and compared to see how they affected the radiated noise during typical approach trajectories. Both wake models share a similar structure that was derived by Beddoes.[27] The vertical wake displacement of the later model was subsequently modified by Leishman[26] to simulate better typical helicopter tip vortex locations in forward flight. These differences in distances of the vortices from the rotor tip-path plane for both wake models are shown in Fig. 6a. The Leishman wake vortices initially stay close to the rotor tip-path plane and then move away with increasing wake age, following the average wake skew angle. Substantial oscillation about a wake skew angle is also present. On average, the Beddoes's wake vortices[27] remain closer to the rotor's tip-path plane (because they have a lower wake skew angle) but oscillate more noticeably about the average.

To see how these effects might influence the BVI noise radiation results, the average acoustic power on the radiation sphere was calculated by the following formula:

$$P_{\text{av}} = 10 \times \log\left[\sum\left\{10^{\text{dB}/10} \times \frac{\Delta A}{A_{\text{sph}}}\right\}\right] \tag{4}$$

The results of this calculation are shown for each wake model as a function of the rotor tip-path-plane angle in Fig. 6b. The general trend of the average radiated noise, first increasing to some maximum value then rapidly decreasing, is the same for both wake models. However, the tip-path-plane angle where this maximum occurs shifts to lower α_{tpp} and the average radiated power becomes less

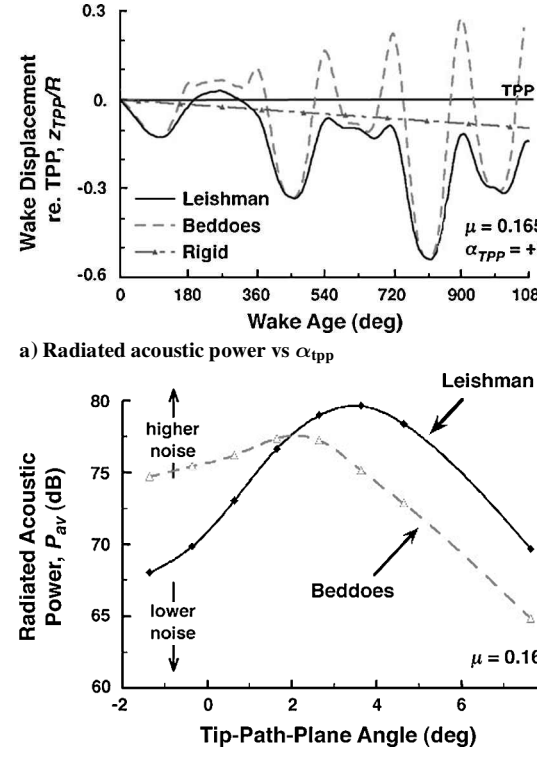

a) Radiated acoustic power vs α_{tpp}

b) Wake geometry

Fig. 6 Comparisons of wake models.

for the Beddoes wake model.[27] The radiated power also does not fall off as quickly from its peak value as the tip-path-plane angle is reduced.

It is clear that the choice of a wake model will influence the specific power that is radiated from each radiation sphere. However, the general trend, of the average power radiating from the sphere reaching a maximum when the rotor tip vortices are close to the rotor, is captured quite well. Therefore, either wake model can be used to see how the flight-path trajectory and control will effect the noise radiated to the ground. The Leishman model[26] was used for the remaining calculations in this paper because it is thought to represent and match experiment better.

The BVI radiation sphere acoustic calculations made, with the helicopter in steady-state trimmed flight, contain the noise information needed for the Q-SAM method. For a given tip-path-plane angle and advance ratio, noise radiation time histories are generated for a period of one rotor revolution for each point on the radiation sphere. Power spectra of these signals are computed and stored in the form of one-third octave band levels, for later reference, as a function of each azimuth and elevation position. This process is repeated until the radiation spheres are developed and stored for all combinations of tip-path-plane angle and advance ratio that the helicopter could possibly encounter during a landing approach.

Some of the predicted BVI acoustics on the radiation spheres are shown in Fig. 7a for the AH-1 helicopter at a constant approach speed of 73 kn ($\mu = 0.165$). For the four different tip-path-plane angles shown, sound pressure level (SPL) contours indicate that the most intense BVI noise occurs when the rotor tip-path-plane angle is between +1.63 and +4.63 deg. In this range of α_{tpp}, the rotor is tilted back such that it is constantly operating in its own wake, hence resulting in small miss distance interactions and stronger BVI noise radiation. At lower and higher values of α_{tpp}, the wake is displaced farther away from the rotor disk. This effectively increases the blade-to-wake miss distance and reduces the radiated BVI noise. There is an associated change in noise directivity shown in Fig. 7a that is the result of the wake intersecting with the rotor farther aft of the rotor disk with increasing tip-path-plane tilt. This allows the older BVIs, formed at regions farther aft on the rotor disk, to dominate with small blade-to-wake miss distances. For this reason, the peak

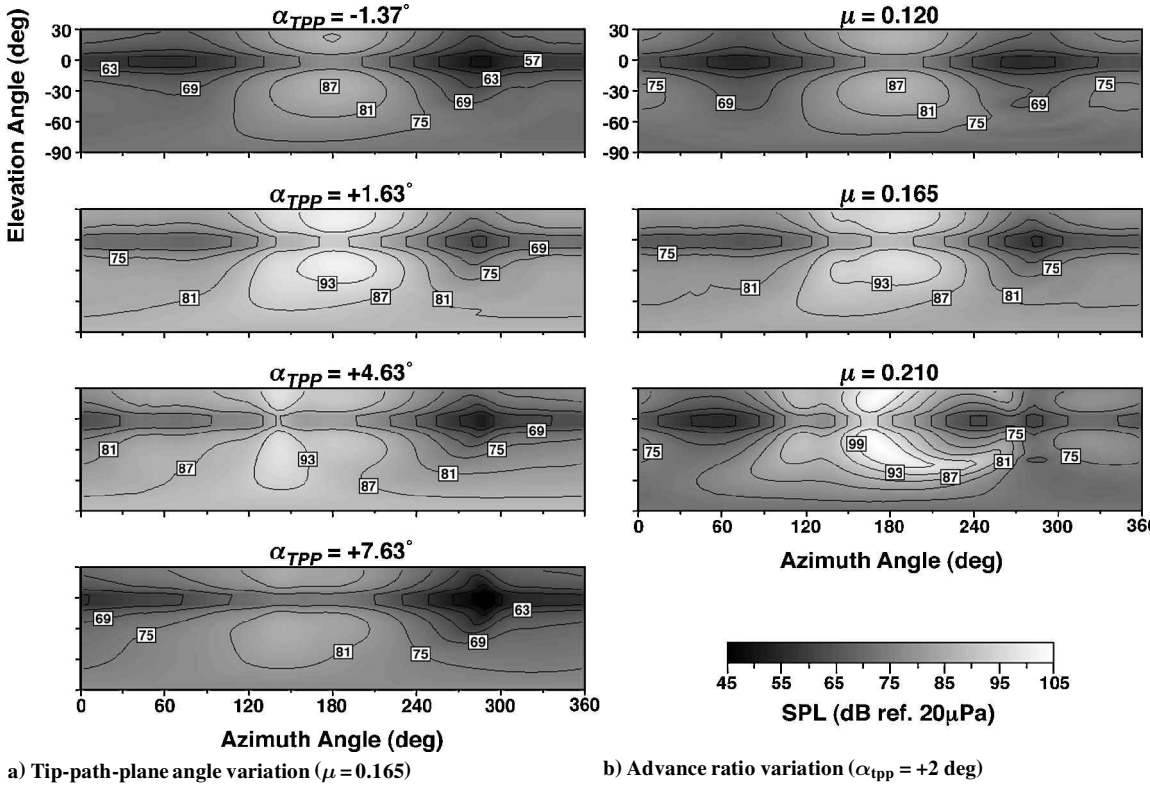

a) Tip-path-plane angle variation ($\mu = 0.165$) b) Advance ratio variation (α_{tpp} = +2 deg)

Fig. 7 Variation of sound pressure levels on radiation spheres.

BVI noise is observed to shift from 180-deg azimuth directly ahead of the rotor (due to the earlier decelerating BVI) to 135-deg azimuth on the advancing side (due to the older broadside BVI).

Similar noise contours are shown in Fig. 7b for an advance ratio sweep with the tip-path-plane angle fixed at +2 deg. The predicted BVI noise levels increase due to the rotor wake moving closer to the tip-path-plane at higher advance ratios. Additional contributions due to strong BVI phasing are found to be important as well. For the advance ratio case of 0.210, this in-phase noise radiation mechanism is found to substantially amplify the BVI noise radiated forward of the rotor.

The amount of acoustic power that is radiated by the rotor is presented in Fig. 8 as a function of α_{tpp} and μ. Rotor tip-path-plane angle α_{tpp} strongly influences the total radiated sound power at all airspeeds. The largest value of sound power occurs at the highest advance ratio, with the peak occurring near $\alpha_{tpp} = +2$ deg. As the advance ratio μ decreases, the peak sound power decreases, and the angle at which it occurs increases.

Based on these calculations, several strategies that minimize radiated sound power are suggested. Negative tip-path-plane tilt reduces BVI noise when the helicopter is descending at low speeds. This mode of operation keeps the rotor wake beneath the rotor, which increases the blade-to-wake miss distance and reduces noise. At higher speed descents, the radiated sound power is reduced by using a large positive tip-path-plane angle to maintain the wake above the rotor plane or by using a negative tip-path-plane tilt to keep the wake below the rotor plane. Some of these noise reduction strategies are explored, in subsequent sections of this paper, with more detail by looking at their effects on measured ground noise.

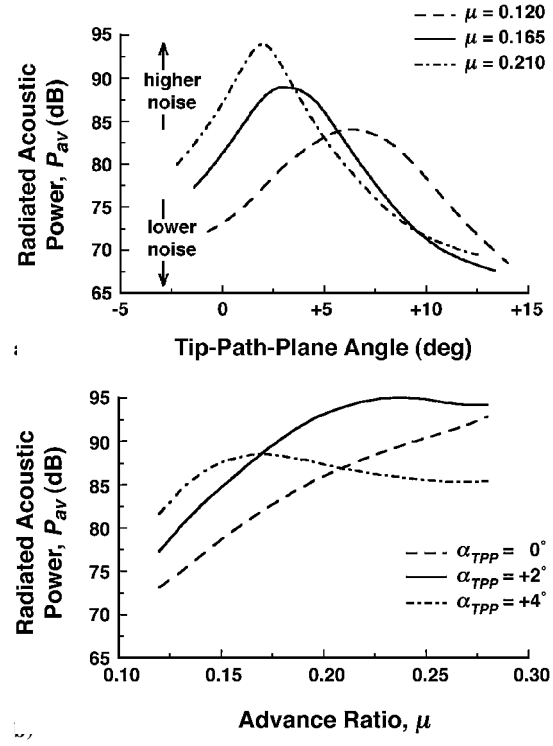

Fig. 8 Variation of average acoustic power on radiation sphere with a) tip-path-plane angle and b) advance ratio.

Ground Noise Mapping Procedure

To implement the Q-SAM method, the helicopter trajectory is divided into a contiguous sequence of trajectory elements. Each element corresponds to the distance traveled by the helicopter in one rotor revolution, that is, $2\pi V/\Omega$. A quasi-static performance state, μ and α_{tpp}, representing an average over that rotor revolution, is assigned to each element. Thus, the trajectory is modeled by a sequence of quasi-static performance states, each lasting one rotor revolution. A no-wind condition is nominally assumed.

Radiation Sphere Selection

The acoustic radiation sphere, described in the preceding section, represents a spherical map of the acoustic power radiated by the helicopter over one rotor revolution. For each element along the trajectory, a radiation sphere that corresponds to the particular μ and α_{tpp} trim state is selected from a predetermined array of spheres tabulated for the entire spectrum of μ and α_{tpp} combinations of interest to the BVI problem. Interpolation is used when the radiation

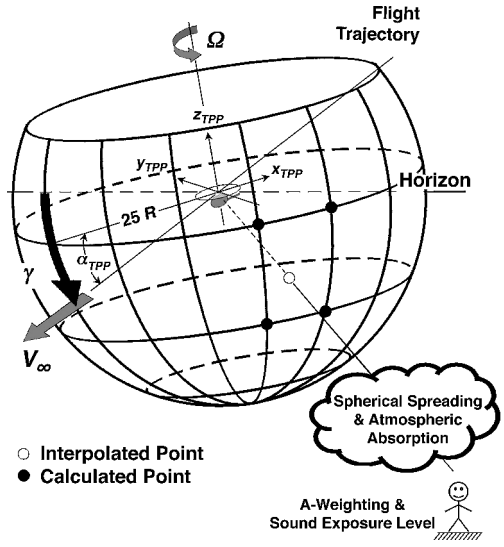

Fig. 9 Acoustics mapping in the Q-SAM method.

sphere at a required μ and α_{tpp} performance state is intermediate (lies between the stored acoustic states) to known computed states.

Mapping Noise to the Ground

With the appropriate radiation sphere obtained for a particular element along the helicopter trajectory, the following steps are taken to map the predicted BVI acoustics on the radiation sphere to the ground.

The radiation sphere is centered at the midpoint of the trajectory and rotated by an angle of $(\gamma + \alpha_{tpp})$ to achieve the correct orientation in physical space. For each observer, a straight line extending from the center of the $25R$ radiation sphere to the observer represents an acoustic ray along which noise is propagated. A two-dimensional linear interpolation is carried out (in the ψ and θ directions), to obtain the one-third octave band levels at the point on the radiation sphere where this ray intersects it (Fig. 9).

To obtain ground noise estimates, the one-third octave band levels are subjected to the effects of spherical spreading and atmospheric sound absorption.[29] (Ground reflection effects are not included in the present analysis.) A dBA level[30] is obtained by applying A weighting and summing up the one-third octave band levels. The dBA level indicates the intensity of the radiated BVI noise received by the observer at one instant in time averaged over one rotor revolution.

To construct the observer time history, Eq. (5) is used to track the arrival time t_{obs} of the individual overall sound pressure levels resulting from the helicoper operating at each element along the trajectory. The source emission time τ_{source} here is approximated by the time when the rotor is at the midinterval of a given trajectory element. With this assumption, R_{obs} represents the seperation distance between this midinterval position and the observer:

$$t_{obs} = \tau_{source} + R_{obs}/a_0 \tag{5}$$

As a final measure of the BVI noise radiation resulting from an associated trajectory, sound exposure levels (SELs) are used to incorporate the effect of time exposure at each ground observer location. The SEL noise metric is calculated from the observer time history using a continuous time integration formulation.[30]

Helicopter Landing Trajectories and Noise Measurement Architecture

The measurement architecture and landing procedures adopted for this study generally follow conventions used in recent Bell Helicopter Textron/NASA flight tests.[31] The trajectories investigated in this paper consist of single approach flight segments, at some prescribed flight-path angle, with either constant speed or small decelerations (up to 0.1 g). The range of descent flight parameters considered are summarized in Table 1.

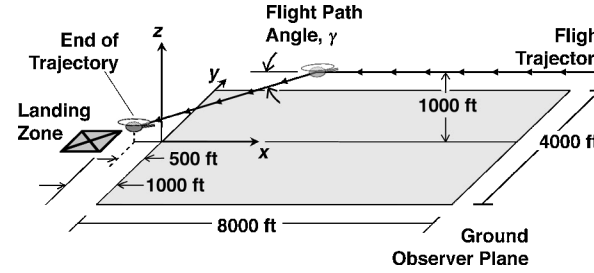

Fig. 10 Helicopter trajectory and ground observer plane.

A rectangular ground observer plane is assumed to lie 1000 ft away from the landing point of the helicopter directly below the flight path (Fig. 10). The observer plane extends to 2000 ft on either side of the trajectory (in the y direction) and is 8000 ft in length (along the x direction). For the calculations in this paper, ground observers are spaced at 55-ft intervals in both the x and y directions.

As shown in Fig. 10, the helicopter is assumed to approach along the centerline ($y = 0$ ft) from the positive x direction. For all of the approach flights considered, it is also assumed that the helicopter is in level flight ($\gamma = 0$ deg) at an altitude of 1000 ft above ground level, before descent. Because the current prediction methods do not simulate the final stages of approach, for example, flare and hover, noise calculations are terminated when the helicopter is 500 ft past the y axis. This stipulation also allows a more complete evaluation of the observer time histories (and the SEL) for observers closest to the termination point of flight. In all cases, both source and observer times are referenced to the zero time, which occurs when the helicopter flies directly over the point $x = 0$, $y = 0$. Negative times correspond to helicopter positions along the approach flight path before the helicopter reaches the 500 ft to landing marker.

Note that, at this present stage of development, the Q-SAM method has some limitations in the prediction of BVI noise while the helicopter is in transition flight. Although changes in trajectory and rotor performance parameters and their rates are usually quite gradual during a normal approach to a landing, the transition from level flight to descent is modeled as an instantaneous change in the helicopter trim state in this paper. This representation produces unphysical discontinuities (switching points) in the predicted observer time histories due to sudden changes in the BVI acoustics. Similar jumps are observed at the transition to and from the decelerating segment of the trajectory. These discontinuities can be removed to some degree by constraining the flight-path angle rate, $|d\gamma/dt|$, and deceleration rate, $|d^2V/dt^2|$, to be less than some specified values. However, the effect of these jumps on the integrated ground noise (SEL) is thought to be small.

Effects of Flight-Path Angle and Advance Ratio

The effect of flight-path angle is shown in Fig. 11 for the AH-1 helicopter at an approach speed of 73 kn ($\mu = 0.165$). SEL contours on the ground observer plane are plotted for various descent angles (negative flight-path angles) ranging from $\gamma = -2$ to -8 deg. Time histories at three specified observers locations are also plotted for comparison; observer A is located at $x = 2200$ ft, $y = -1100$ ft (on the retreating side), observer B at $x = 2200$ ft, $y = 0$ ft directly below the flight path, and observer C at $x = 2200$ ft, $y = 1100$ ft (on the advancing side).

For all of these trajectories and at all of the performance states encountered, the radiation spheres are oriented identically with respect to the horizon. This is because $(\gamma + \alpha_{tpp})$ is only a function of the helicopter drag, which remains constant for a given advance ratio [Eq. (3)]. Differences in ground noise patterns for these different descent angles reflect changes in directivity and noise levels on the radiation spheres, as well as the effect of trajectory variations (distance and directivity effects), A weighting, and atmospheric sound absorption. In general, higher SEL values are observed near $x = 0$ ft,

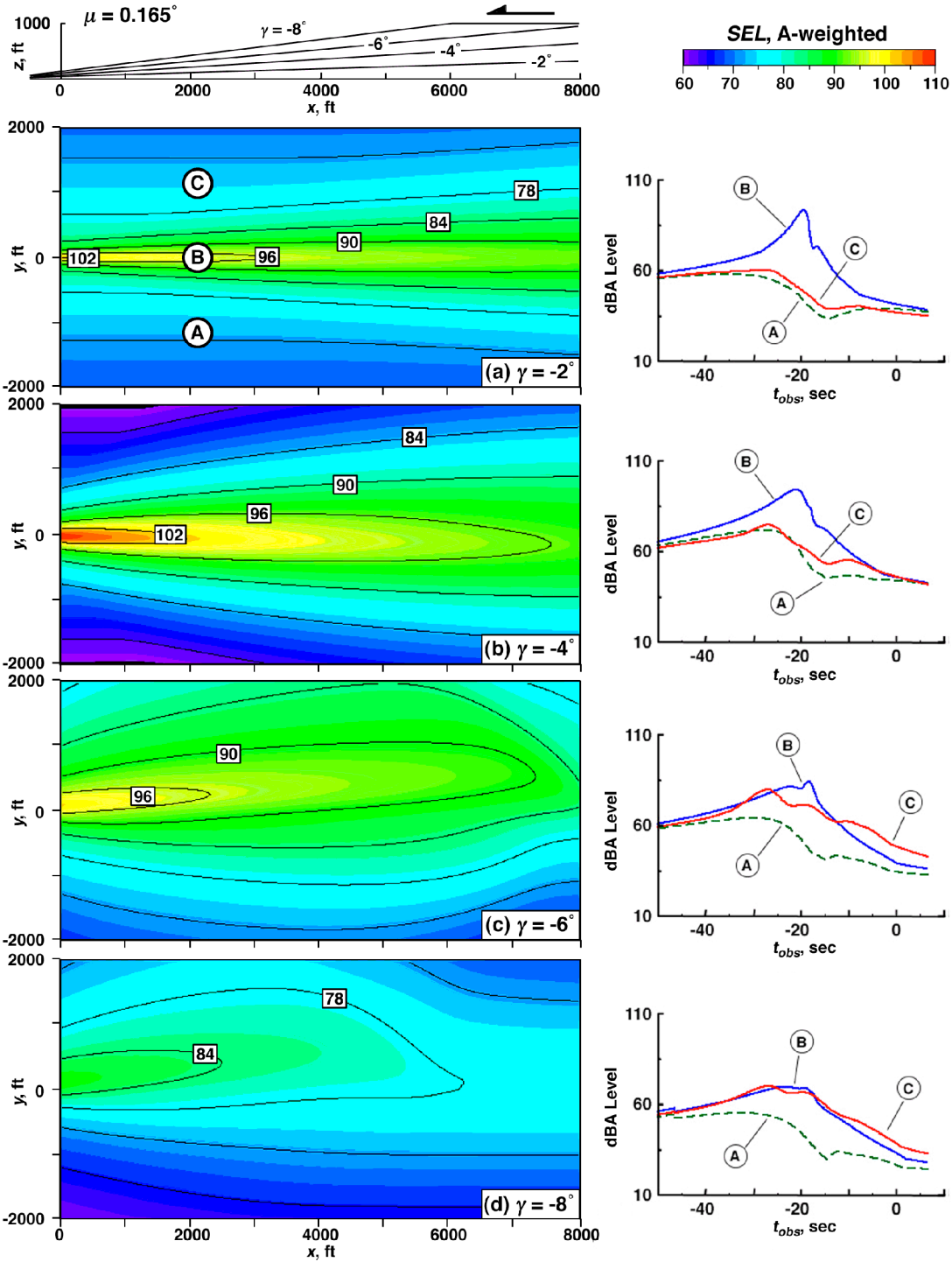

Fig. 11 Predicted SEL ground noise contours and acoustic time histories for $\mu = 0.165$ at four different flight path angles; $\gamma = -2, -4, -6$, and -8 deg.

$y = 0$ ft directly below the flight path because of closer proximity to the trajectory.

The concept of average rotor inflow [Eq. (6)] explains some of the predicted noise trends shown in Fig. 11. This concept and its application to BVI noise have been studied in some detail in Ref. 12. In general, strong positive and negative inflow pushes the rotor wake farther away from the rotor disk, which reduces the likelihood of close BVIs that radiate strong BVI noise. When the average inflow is near zero, the rotor wake remains mostly in the rotor tip-path-plane, which increases BVI noise radiation,

$$\lambda = (V \sin \alpha_{\text{tpp}} - v)/\Omega R \tag{6}$$

For all of the descent cases shown in Fig. 11, the radiated noise from the level flight segment ($\gamma = 0$, $\alpha_{\text{tpp}} = -1.37$ deg) is found to be quite small. This is because in level flight, both the $V \sin \alpha_{\text{tpp}}$ term and the rotor-induced-velocity term combine to form a strong negative inflow (downwash) that displaces the wake farther below the rotor and reduces BVI. Some indications to this effect are also shown in Fig. 7a for the radiation sphere acoustics predicted at this trim state.

When the helicopter is in descent, the negative flight-path angle (descent angle) tends to make the tip-path-plane angle more positive [Eq. (3)]. The positive $V \sin \alpha_{\text{tpp}}$ term in Eq. (6) may become strong enough to negate the effects of the negative rotor-induced velocity. At very shallow descent angles ($\gamma = -2$ deg, $\alpha_{\text{tpp}} = +0.63$ deg) the average inflow remains negative, which helps to keep the wake underneath the rotor. As the helicopter descends at a steeper angle ($\gamma = -4$ deg, $\alpha_{\text{tpp}} = +2.63$ deg), the tip-path-plane angle tips farther

back and the wake moves close to the plane of the rotor. The rotor inflow approaches zero as the $V \sin \alpha_{tpp}$ contribution becomes more positive. Consequently, the highest ground noise is predicted for this descent approach (Fig. 11b). For even steeper descents ($\gamma = -6$ and -8 deg), α_{tpp} becomes large enough (positive) to override the effect of a negative average-induced velocity. The net rotor inflow becomes positive which pushes the wake above the rotor to increase the BVI miss distances and reduces noise (Figs. 11c and 11d).

Also notice that the SEL contours becomes asymmetric (with respect to the flight line) with steeper descents. This change in ground noise pattern signifies a different BVI directivity as a result of the greater (more positive) tip-path-plane tilt that emphasizes the miss distance effect of the older BVI formed farther aft of the rotor, which radiates more asymetrically.[28] The transition to asymmetry is observed to occur after conditions corresponding to when the peak BVI noise is radiated (γ is steeper than -4 deg). The predicted observer time histories for all of these different descents exhibit similar increasing and decreasing noise trends. This variation in the noise received by a ground observer is not only due to the proximity of the helicopter, but also the directivity of the radiated BVI noise at the particular performance state. In general, the same trends observed in the SEL contour plots are also observed for the time histories shown in Fig. 11. However, the observer time histories show much greater detail and, therefore, enable a better understanding of the BVI noise radiation at different flight trajectory settings.

For example, it can be observed that at shallow approaches, the time histories have sharper peaks compared to the time histories predicted for steeper descents. This variation is likely to be due to the increased distance between the observer and the helicopter at steeper descents. The discontinuity in time history (Fig. 11d) at $t_{obs} = -46.5$ s represents the switch from level flight to descent. Similar trends in the SEL contours and acoustic time histories are predicted at other flight velocities as well.

Effect of *X*-Force

The effect of an aerodynamic X-force (drag) device on radiated BVI noise is shown in Figs. 12a and 12b for a flight speed of 93 kn ($\mu = 0.210$) at two different descent angles ($\gamma = -3$ and $\gamma = -9$ deg). Ground noise profiles are compared for trajectories with and without the addition of X force at the same constant flight speed and the same descent angles. For these calculations, the added X force is assumed to double the effective drag on the AH-1 helicopter.

As shown in Eq. (3), the addition of X force effectively makes the tip-path-plane angle more negative (by -2.2 deg at the 93-kn cases shown in Fig. 12). At shallow descent angles, the use of X force is shown to be an effective noise reduction technique (Fig. 12a). Under negative or near-zero inflow conditions (wake below or near the plane of the rotor), applying X force tilts the tip-path-plane more negatively and increases negative rotor inflow. This net downwash pushes the vortices farther down below the rotor plane to separate the BVI miss distance. The associated BVI noise reduction is shown in Fig. 12a.

The effect of X force at steep descent angles (positive inflow conditions) is quite the opposite. In such cases, applying a negative tip-path-plane angle brings the wake closer to the rotor blades. As observed in Fig. 12b for a -9-deg approach, this reduces the miss distances of the interactions and increases the likelihood of high BVI noise

The use of an aerodynamic X force is, therefore, beneficial at high speeds and shallow flight-path angles. At lower speeds, the aerodynamic control is less effective. For shallow descent at low speeds, a nonaerodynamic X force control[12] should be a more attractive noise reduction strategy.

Effect of Deceleration Parallel to the Flight Path

From the quasi-static performance model discussed before, deceleration causes the tip-path-plane to tilt back making it more positive [Eq. (3)]. A deceleration of 0.1 g corresponds to a $+5.7$-deg increase in tip-path-plane angle. This change in the tip-path-plane angle can drastically alter BVI noise radiation levels, as shown in Fig. 8a. When applied to performance states that correspond to peak noise radiation (near zero inflow or small inflow conditions) or positive inflow (wake above the rotor), this quasi-static control variable effectively reduces noise radiation, by making the inflow more positive and pushing the wake farther above the rotor. When operating in a negative inflow region (wake below the rotor), a small deceleration parallel to the flight path tends to make the inflow more positive,

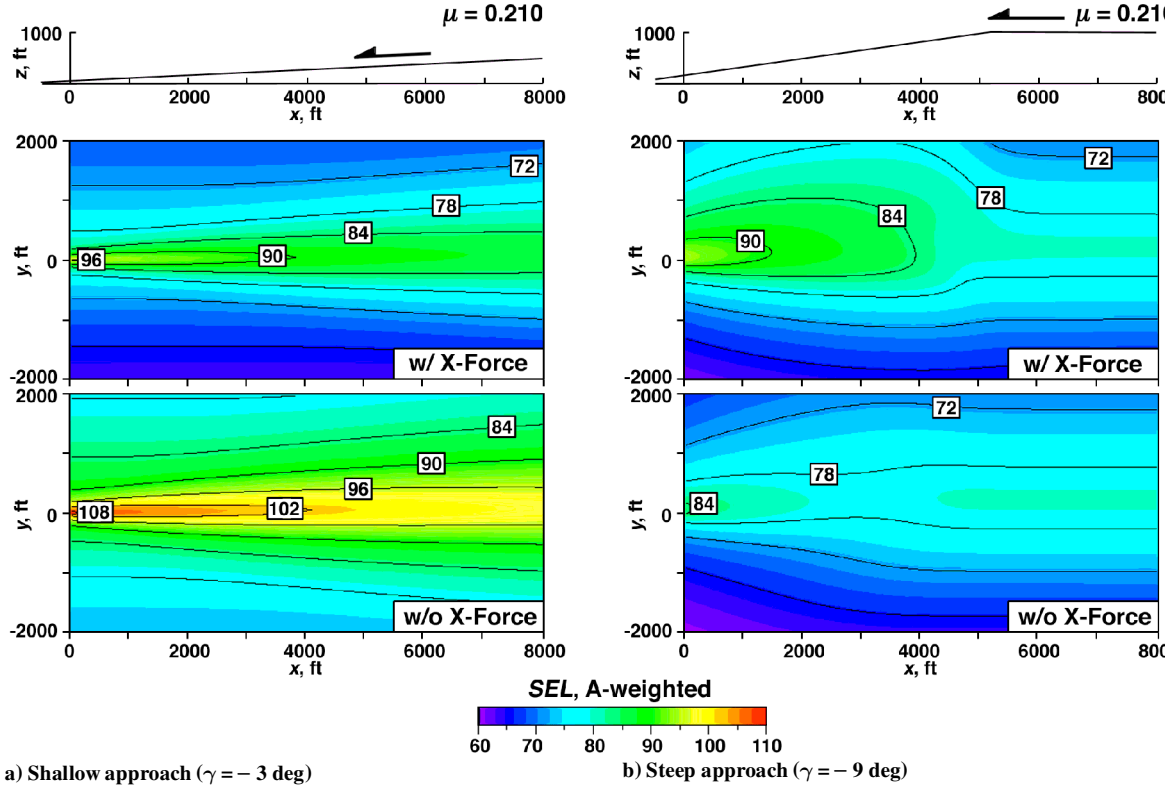

a) Shallow approach ($\gamma = -3$ deg) b) Steep approach ($\gamma = -9$ deg)

Fig. 12 Predicted SEL ground noise with and without *X*-force.

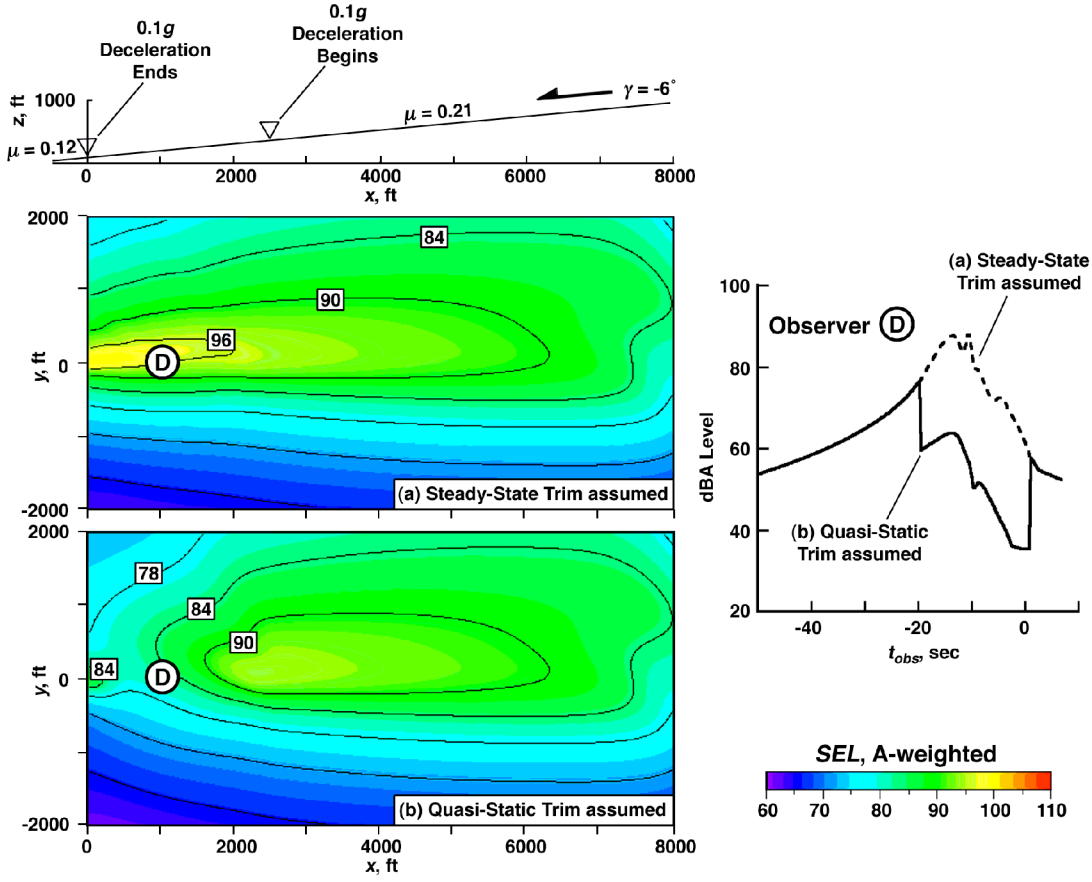

Fig. 13 Effect of deceleration for a − 6-deg descent.

pushing the wake close to the plane of the rotor and, thus, increasing the likelihood of BVI noise.

The effect of deceleration is shown in Fig. 13 for a nominal descent angle of −6 deg. The deceleration is assumed to end when the helicopter is directly above the point $x = 0$ ft, $y = 0$ ft. The helicopter flies at 93 kn ($\mu = 0.21$) during level flight and then descends at the same speed, at a flight-path angle of −6 deg. It decelerates to a speed of 53 kn ($\mu = 0.12$) and then descends at constant speed till the final point along the trajectory (500 ft from the landing point) is reached. The deceleration segment is assumed to end at the point on the trajectory directly above the point $x = 0$ ft, $y = 0$ ft.

Treating the deceleration segment of the trajectory as a sequence of steady-state performance states with constant speeds corresponding to those encountered during the actual deceleration does not account for changes in tip-path-plane angle due to the deceleration term [Eq. (3)]. In Fig. 13a, the sound exposure levels on the ground based on steady-state trim assumptions ($A_x = 0$), are compared with results obtained using quasi-static performance assumptions for a deceleration of 0.1 g (Fig. 13b). The latter is more representative of the actual performance state of the rotor in decelerating flight, albeit in a quasi-static sense, because steady assumptions ignore the effect of deceleration on tip-path-plane angle. Therefore, it is not surprising that the steady-state approach overpredicts noise radiation levels and fails to demonstrate the efficacy of using deceleration as a noise reduction technique. Current calculations show an overprediction of BVI SEL values by more than 15 dB for some ground observers close to the deceleration portion segment of the flight path.

The dBA time histories corresponding to the steady-state trim and the quasi-static trim assumptions are presented in Fig. 13. An observer D, located directly below the flight path at $x = 1100$ ft is used to highlight the differences in the results obtained. The use of steady-state trim predicts higher BVI noise radiation (dashed line). The observer time history predicted by quasi-static trim (solid line) is characterized by a low-noise bucket, which indicates a very quiet flight while the helicopter is undergoing deceleration. The two switching points correspond to discontinuities resulting from the transition to and from the beginning and the end of the deceleration phase, respectively. Because deceleration reduces the BVI noise so effectively, the peak noise predicted at this observer is due to the constant speed (93 kn) flight segment prior to deceleration.

Figures 14a and 14b show the SEL distributions and dBA time histories for three observers on the ground plane. Two trajectories with 0.05- and 0.10-g deceleration are considered with the helicopter beginning deceleration at 93 kn ($\mu = .21$) and terminating at 53 kn ($\mu = 0.12$). Both of these cases are evaluated with quasi-static trim and show significant reduction in BVI noise when compared to the ground noise contour for a nominal approach at 73 kn ($\mu = 0.165$) and −6-deg descent angle (Fig. 11c). The 0.05-g deceleration (Fig. 14a) appears to offer more BVI noise reduction benefits with a wider spread of low noise regions compared to the 0.1-g deceleration. However, the predicted time histories for several observers situated directly underneath the flight path indicates a greater degree of noise reduction at 0.1-g deceleration. Some of this noise reduction may not be reflected in the SEL contours as a result of the strong BVI noise radiation from the constant speed descent flight segment before deceleration. Nonetheless, the effect of deceleration is shown here to be very effective in reducing the BVI ground noise from a helicopter in descent.

Although not considered in this initial calculation, the deceleration flight can be executed at different positions along the trajectory to target its noise reduction at some communities that are more noise sensitive. Also not considered are the effects of realistic flight constraints, such as the acceptable limits of deceleration and the rate of change of deceleration. These effects are important for the handling qualities of the vehicle and require more research before incorporating deceleration as a trajectory control parameter to reduce noise.

Suggested Low Noise Trajectories

It is shown in Figs. 11–14 and in Ref. 12 that one of the key to reducing BVI noise is to avoid the rotor interacting closely its own

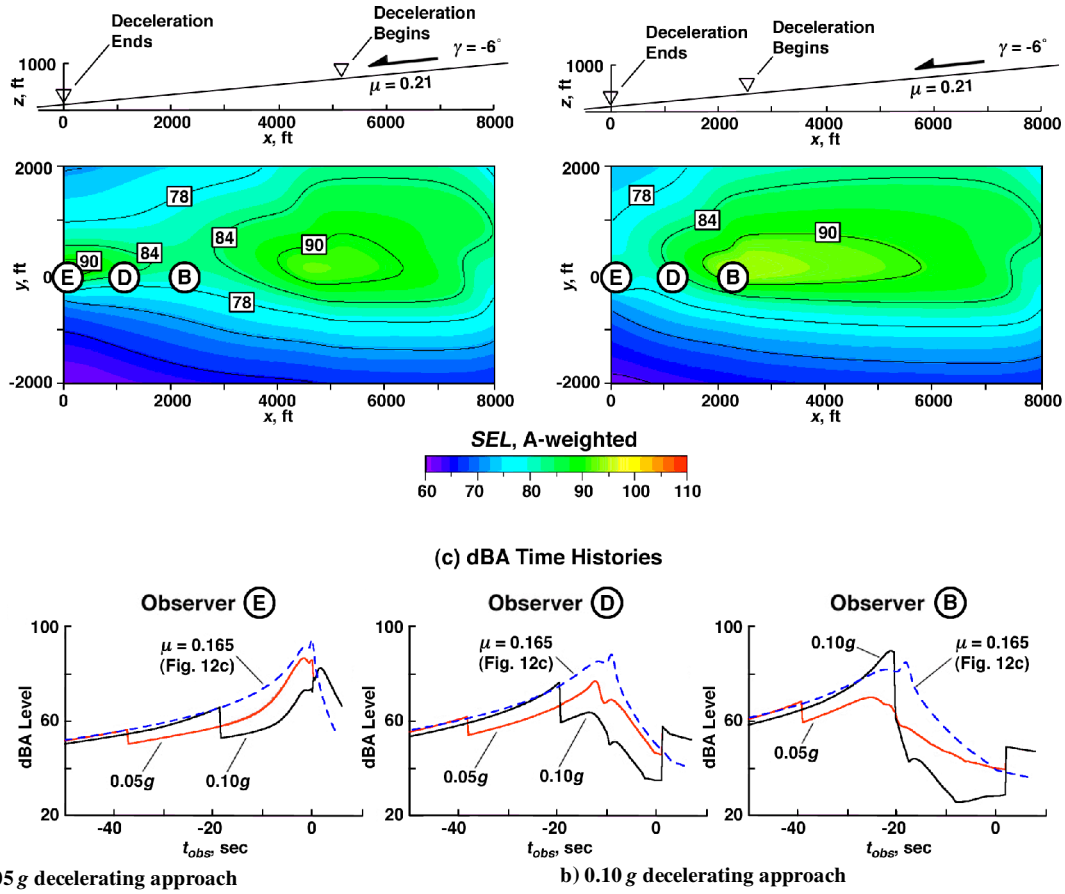

a) 0.05 g decelerating approach b) 0.10 g decelerating approach

Fig. 14 Effect of different deceleration for a − 6-deg descent.

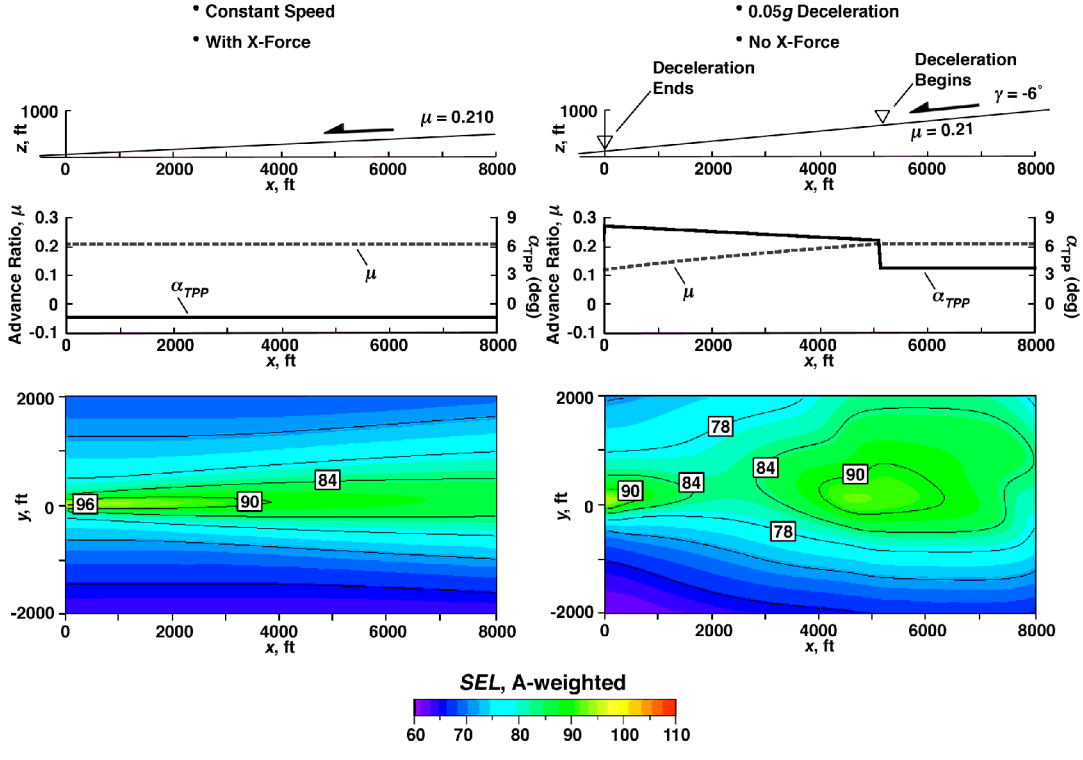

a) Shallow approach ($\gamma = -3$ deg), constant speed and with X force b) Normal approach ($\gamma = -6$ deg) 0.05-g deceleration and no X force

Fig. 15 Performance states and predicted ground noise for suggested low noise trajectories.

wake. Applying the appropriate X-force controls and decelerations for selected approach trajectories are found to capitalize on this effect of distancing the wake from the rotor to reduce BVI noise radiation. Depending on the state of the helicopter, this can be achieved either by enforcing a negative tilt-path-plane tilt that displaces the wake farther under the rotor or by a positive tip-path-plane tilt that keeps the wake above the rotor.

These findings are formulated in Fig. 15 as two viable low noise trajectories. Figure 15a demonstrates the use of X-force controls as an effective means to fly the helicopter quietly while approaching to land at a shallow descent angle ($\gamma = -3$ deg). With X force, the tip-path plane of the rotor is forced to tilt farther forward to maintain trim. This effectively results in an additional negative inflow component pushing the wake that already exists below the rotor even farther downward. The larger separation distance between the rotor blades and the wake reduces the likelihood of strong BVI.

At a steeper descent of -6 deg (Fig. 15b), the use of small decelerations is found to yield a quieter ground noise profile. Deceleration increases the rotor tip-path-plane angle and the positive inflow through the rotor disk. With the wake residing primarily near or above the rotor tip-path plane, the additional positive inflow contribution due to deceleration draws the wake farther above and away from the rotor disk. This increase in blade-to-wake miss distance reduces the intensity of radiated BVI noise.

Although these examples here are for the AH-1 helicopter, the principles of achieving low BVI noise radiation using the trajectory and control parameters can be applied in general for all rotorcraft. The actual implementation and/or selection of flight trajectory, X-force device, and deceleration are, however, case specific and need(s) further study, experimentation, and refinement.

Conclusions

A new method, Q-SAM, and its associated computational procedure has been developed to predict rotorcraft external noise. The Q-SAM method relies on an expansion of the nondimensional force equations about steady-state trimmed flight to account for changes in the vehicles noise radiation patterns resulting from different trajectory and flight-path control settings (flight-path angle, advance ratio, X force, and acceleration parallel to the flight path).

The Q-SAM method can replace direct calculation of the noise from the vehicle performance/aerodynamic and acoustic equations. The new method first acquires and stores external noise as a function of the helicopter's steady-state trim variables. The acquisition of the noise data can be obtained experimentally or theoretically. These patterns, which are unique for each helicopter, are adjusted for changes from steady-state trim and used to project noise to the acoustic far field. This ability to measure steady-state radiation patterns and then map the patterns has been shown to facilitate validation and understanding of the noise radiation process for the AH-1 helicopter. The complex aerodynamics that are integral to the prediction of BVI noise are implicitly captured by the Q-SAM method.

Parametric changes in flight-path angle and advance ratio have shown that steady-state BVI noise radiation can reach local maxima over this parameter space. Flying quietly by choosing the correct flight-path angle and advance ratio are likely to yield two different minimum noise flight profiles: a steep medium velocity approach or a shallow lower velocity approach profile.

Helicopter acceleration or deceleration parallel to the flight path during landing/approach conditions has a strong influence on external BVI noise radiation. Predicting BVI noise along a changing velocity trajectory without including the effect of acceleration may result in large miscalculations of BVI noise radiation and, consequently, may result in large miscalculations of ground noise.

For the AH-1 helicopter, these calculations have shown that deceleration is effective at reducing BVI noise during steep approaches. For steep approaches, deceleration effectively increases the miss distances of the shed vortices by positioning them at greater distances above the rotor tip-path plane. The increased miss distance decreases the level and frequency content of the ground noise predictions of noise level and annoyance. The steep approaches, however, also have a tendency to spread acoustic energy to the sides of the flight path.

X-force control is also shown to reduce ground BVI noise exposure for the AH-1 helicopter in some flight conditions. It is most effective at shallow approach angles when the helicopter has zero deceleration. With these more shallow approaches, areas of high noise levels are generally confined to positions directly under the flight path. The choice of a shallow trajectory might be useful for heliports that allow approaches along noise insensitive corridors.

The Q-SAM method has shown that reducing BVI noise radiation for this two-bladed helicopter is a complex problem that depends on the noise radiation characteristics of the helicopter and judicious use of flight-path and configuration controls. The method qualitatively explains many of the experimental observations over the years about how to fly quietly. Use of control theory to determine the benefits and to explore the limits of the Q-SAM method is a logical next step in this research.

Acknowledgments

The authors thank Bryan Edwards (Bell Helicopter Textron) and Robert Chen (NASA Ames Research Center) for their valuable guidance and support. The authors also acknowledge the insightful discussions with J. G. Leishman and J. D. Baeder, as well as J. Sitaraman and M. Dhingra, at the University of Maryland.

References

[1] Schmitz, F. H., "Rotor Noise," *Aeroacoustics of Flight Vehicles, Theory and Practice*, edited by H. H. Hubbard, Vol. 1, Noise Sources, Acoustical Society of America, New York, 1995, pp. 65–149.

[2] George, A. R., "Helicopter Noise: State of the Art," *Journal of Aircraft*, Vol. 15, No. 11, 1978, pp. 707–715.

[3] Boxwell, D. A., Schmitz, F. H., Splettstoesser, W. R., and Schultz, K. J., "Helicopter Model Rotor–Blade Vortex Interaction Impulsive Noise: Scalability and Parametric Variations," *Journal of the American Helicopter Society*, Vol. 32, No. 1, 1987, pp. 3–12.

[4] Shultz, K. J., and Splettstoesser, W. R., "Measured and Predicted Impulsive Noise Directivity Characteristics," Thirteenth European Rotorcraft Forum, Paper 12, Sept. 1987.

[5] Tung, C., Kube, R., Brooks, T. F., and Rahier, G., "Prediction and Measurement of Blade–Vortex Interaction," *Journal of Aircraft*, Vol. 35, No. 2, 1998, pp. 260–266.

[6] Hawles, D. R., "Flight Operations to Minimize Noise," *Vertiflite*, Vol. 17, No. 2, 1971, pp. 4–9.

[7] "Pilot Training," *Fly Neighborly Guide*, Helicopter Association International (HAI) Fly Neighborly Committee, Alexandria, VA, 1993, pp. 3–26.

[8] Hindson, W. S., and Chen, R. T. N., "Operational Tests of Noise Abatement for Rotorcraft Using Differential GPS for Guidance," *Journal of the American Helicopter Society*, Vol. 43, No. 4, 1998, pp. 352–359.

[9] Schmitz, F. H., Stepniewski, W. Z., Gibs, J., and Hinterkeuser, E., "A Comparison of Optimal and Noise-Abatement Trajectories of a Tilt-Rotor Aircraft," NASA CR-2034, May 1972.

[10] Stepniewski, W. Z., and Schmitz, F. H., "Possibilities and Problems of Achieving Community Noise Acceptance of VTOL Aircraft," *Aeronautical Journal of Great Britain*, Vol. 77, No. 730, 1973, pp. 311–326.

[11] Schmitz, F. H., and Stepniewski, W. Z., "Reduction of VTOL Operational Noise Through Flight Trajectory Management," *Journal of Aircraft*, Vol. 10, No. 7, 1973, pp. 385–394.

[12] Schmitz, F. H., "Reduction of Blade–Vortex Interaction (BVI) Noise through X-Force Control," *Journal of the American Helicopter Society*, Vol. 43, No. 1, 1998, pp. 14–24.

[13] Abello, J. C., and George, A. R., "Rotorcraft BVI Noise Radiation by Attitude Modification," AIAA Paper 99-1931, May 1999.

[14] Lucas, M. J., and Marcolini, M. A., "Rotorcraft Noise Model," American Helicopter Society Technical Specialists Meeting on Rotorcraft Acoustics and Aerodynamics, Oct. 1997.

[15] Sim, B. W., and Schmitz, F. H., "Acoustic Phasing and Amplification Effects of Single Rotor Helicopter Blade–Vortex Interactions," American Helicopter Society 55th Annual Forum, May 1999.

[16] Lowson, M. V., "Focusing of Helicopter BVI Noise," *Journal of Sound and Vibration*, Vol. 190, No. 3, 1996, pp. 477–494.

[17] Leishman, J. G., "Acoustic Focusing Effects Generated by Parallel and Oblique Blade Vortex Interactions," American Helicopter Society Technical Specialists Meeting on Rotorcraft Acoustics and Aerodynamics, Oct. 1997.

[18] Schmitz, F. H., and Sim, B. W., "Radiation and Directionality Characteristics of Advancing Side Blade–Vortex Interaction (BVI) Noise," AIAA Paper 2000-1922, June 2000.

[19]Sim, B. W., and Schmitz, F. H., "Blade–Vortex Interaction (BVI) Noise: Retreating Side Characteristics, Sensitivity to Chordwise Loading and Unsteady Aerodynamics," American Helicopter Society Aeromechanics Specialists Meeting, Nov. 2000.

[20]Johnson, W., "Airloads and Wake Models for a Comprehensive Helicopter Analysis," NASA CR-177551, April 1990.

[21]Bir, G., and Chopra, I., "University of Maryland Advanced Rotorcraft Code (UMARC), Theory Manual," Rept. UM-AERO 94-18, Univ. of Maryland, College Park, MD, 1994.

[22]Ffowcs-Williams, J. E., and Hawkings, D. L., "Sound Generation by Turbulence and Surfaces in Arbiturary Motion," *Philosophical Transactions of the Royal Society*, Vol. A 264, No. 1151, 1969, pp. 321–342.

[23]Farassat, F., "Linear Acoustic Formulas for Calculation of Rotating Blade Noise," *AIAA Journal*, Vol. 19, No. 9, 1981, pp. 1122–1130.

[24]Brentner, K. S., and Jones, H. E., "Noise Prediction for Maneuvering Rotorcraft," AIAA Paper 2000-2031, June 2000.

[25]Sim, B. W., Schmitz, F. H., and Aoyama, T., "Near/Far-Field Radiation Characteristics of Advancing Side Helicopter Blade-Vortex Interaction (BVI) Noise," American Helicopter Society 56th Annual National Forum, May 2000.

[26]Leishman, J. G., "Rotor Wakes and Tip Vortices," *Principles of Helicopter Aerodynamics*, 1st ed., Cambridge Univ. Press, Cambridge, England, U.K., 2000, pp. 418–486.

[27]Beddoes, T. S., "A Wake Model for High Resolution Airloads," Army Research Office 2nd International Conf. on Rotorcraft Basic Research, Research Triangle Park, NC, Feb. 1985.

[28]Lowson, M. V., "The Sound Field for Singularities in Motion," *Proceedings of the Royal Aeronautical Society*, Vol. 286, 1965, pp. 559–572.

[29]"Method for Calculation of the Absorption of Sound by the Atmosphere," American National Standard, ANSI S1.26-1995, American National Standard Inst., NY, 1995.

[30]Bennet, R. L., and Pearsons, K. S., "Handbook of Aircraft Noise Metric," NASA CR-3406, 1981.

[31]Conner, D. A., Marcolini, M. A., Decker, W. A., Cline, J. H., Edwards, B. D., Nicks, C. O., and Klein, P. D., "XV-15 Tiltrotor Low Noise Approach Operations," American Helicopter Society 55th Annual Forum, May 1999.